High order finite difference methods with subcell resolution for stiff multispecies detonation capturing

Wei Wang[*], Chi-Wang Shu[†], H. C. Yee[‡], Dmitry V. Kotov[§] and Björn Sjögreen[¶]

July 12, 2014

Abstract

In this paper, we extend the high order finite-difference method with subcell resolution (SR) in [34] for two-species stiff one-reaction models to multispecies and multireaction chemical reactive flows, which are significantly more difficult because of the multiple scales generated by different reactions. For reaction problems, when the reaction time scale is very small, the reaction zone scale is also small and the governing equations become very stiff. Wrong propagation speed of discontinuity may occur due to the underresolved numerical solution in both space and time. The present SR method for reactive Euler system is a fractional step method. In the convection step, any high order shock-capturing method can be used. In the reaction step, an ODE solver is applied but with certain computed flow variables in the shock region modified by the Harten subcell resolution idea. Several numerical examples of multispecies and multireaction reactive flows are performed in both one and two dimensions. Studies demonstrate that the SR method can capture the correct propagation speed of discontinuities in very coarse meshes.

Key words: stiff reaction term, shock capturing, detonation, WENO, ENO subcell resolution, multispecies, multireactions

[*]Department of Mathematics and Statistics, Florida International University, Miami, FL 33199. E-mail: weiwang1@fiu.edu. Research supported by NASA grant NNX12AJ62A.

[†]Division of Applied Mathematics, Brown University, Providence, RI 02912. E-mail: shu@dam.brown.edu. Research supported by NASA grant NNX12AJ62A and NSF grant DMS-1112700.

[‡]NASA Ames Research Center, Moffett Field, CA 94035. E-mail: helen.m.yee@nasa.gov. Research supported by DOE/SciDAC SAP grant DE-AI02-06ER25796.

[§]Center for Turbulence Research, Stanford, CA 94305. E-mail: dkotov@stanford.edu. Research supported by DOE/SciDAC SAP grant DE-AI02-06ER25796.

[¶]Lawrence Livermore National Laboratory, Livermore, CA 94551. E-mail: sjogreen2@llnl.gov.

1 Introduction

When simulating high speed reactive flows, a wide range of reaction rates may be present, and the chemical time-scales are often orders of magnitude smaller than the typical relaxation time of fluid dynamics, leading to the stiffness of the problem.

The mathematical model for chemical reactive flows can be described by the reactive Euler equations coupled with source terms. Consider the reactive Euler equations in two dimensions in the form

$$U_t + F(U)_x + G(U)_y = S(U), \tag{1}$$

where U, $F(U)$, $G(U)$ and $S(U)$ are vectors. If the time scale of the ordinary differential equation (ODE) $U_t = S(U)$ for the source term is orders of magnitude smaller than the time scale of the homogeneous conservation law $U_t + F(U)_x + G(U)_y = 0$ then the problem is said to be stiff. In high speed chemical reacting flows, the source term represents the chemical reactions which may be much faster than the gas flow. This leads to problems of numerical stiffness. Insufficient spatial resolution may cause an incorrect propagation speed of discontinuities and nonphysical states for standard dissipative numerical methods.

This numerical phenomenon was first observed by Colella et al. [12] in 1986 who considered both the reactive Euler equations and a simplified system obtained by coupling the inviscid Burgers equation with a single convection/reaction equation. LeVeque and Yee [22] showed that a similar spurious propagation phenomenon can be observed even with scalar equations, by properly defining a model problem with a stiff source term.

Numerically resolving all the chemical small scales will result in tremendous computational cost. Therefore, many works have contributed to the analysis and development of underresolved numerical methods which are able to capture the correct shock/discontinuities location and speed without resolving the small chemical scales. Examples include the level set and front tracking methods [23, 19, 6, 26, 30], random choice method [10, 11, 12, 24], random projection method [1, 2, 3] and many other works [4, 27, 5, 31, 7, 14, 8, 9, 13, 16, 32, 25, 17]. See Wang et al. [33] for a comprehensive overview of the last two decades of this development. Wang et al. [33] also proposed a new high order finite difference method with subcell resolution for advection equations with stiff source terms for a single reaction to overcome the difficulty.

In this work, we extend the subcell resolution method to multispecies and multireaction problems, which are significantly more difficult because of the multiple scales generated by different reactions. The proposed SR method for the reactive Euler system is a fractional step method. In the convection step, any high order shock-capturing method can be used. However shock-capturing schemes will produce transition points due to the numerical dissipation. Here, transition points mean the smeared numerical solution in the shock region. In the reaction step, an ODE solver is applied but with

the values of certain computed flow variables at the transition points in the shock region modified by a reconstructed polynomial using the idea of Harten's subcell resolution method. Here, we only address the issue in developing methods to obtain the correct propagation speed of discontinuities using a coarse grid without resolving the detonation peak correctly as the width of the detonation front consists of 1-2 grid points only.

2 Review of the method for 1D scalar problems

We first review the finite difference method with subcell resolution (SR), introduced in [34] for the scalar model problem in [22].

Consider

$$u_t + f(u)_x = S(u), \tag{2}$$

$$S(u) = -\mu u\,(u-\alpha)\,(u-1), \tag{3}$$

with the initial condition

$$u(x,0) = \begin{cases} 1, & x \le x_0 \\ 0, & x > x_0 \end{cases}, \tag{4}$$

where α is a parameter, $0 < \alpha < 1$, and x_0 is the position of the initial discontinuity.

The SR method uses a fractional step approach. The numerical solution at time level t_{n+1} is approximated by

$$u^{n+1} = R(\Delta t)A(\Delta t)u^n. \tag{5}$$

The convection operator A is defined to approximate the solution of the homogeneous part of the problem on the time interval, i.e.,

$$u_t + f(u)_x = 0, \quad t_n \le t \le t_{n+1}. \tag{6}$$

The reaction operator R is defined to approximate the solution on a time step of the reaction problem:

$$\frac{du}{dt} = S(u), \quad t_n \le t \le t_{n+1}. \tag{7}$$

In the Strang-splitting in [29], the numerical solution at time step t_{n+1} is computed by

$$u^{n+1} = A\left(\frac{\Delta t}{2}\right) R(\Delta t) A\left(\frac{\Delta t}{2}\right) u^n, \tag{8}$$

where the convection operator is over a time step Δt and the reaction operator is over $\Delta t/2$. This strategy improves the time accuracy to second order. The two half-step reaction operations over adjacent time steps can be combined to save cost.

Any high resolution shock capturing operator can be used in the convection step. The purpose in this step is to minimize the transition points in the shock region, but

not to remove them completely (which is not realistic). In this paper, we use the fifth-order finite difference WENO schemes [20] with a third-order TVD Runge-Kutta time discretization.

In the convection step, we apply an ODE solver with Harten's subcell resolution technique. The procedure can be summarized in the following steps:

(1) Use a "shock indicator" to identify cells in which discontinuities are believed to be situated. We consider the following minmod-based shock indicator in [15, 28]. Let

$$s_i = \text{minmod}\{u_{i+1} - u_i, u_i - u_{i-1}\}, \tag{9}$$

define the cell I_i as troubled if $|s_i| \geq |s_{i-1}|$ and $|s_i| \geq |s_{i+1}|$, with at least one being a strict inequality. Notice that this troubled cell-identifying method will only find the "worst" cell inside a shock transition. That is, if there are several consecutive transition cells, only the worst one will be identified as a troubled cell.

(2) In a troubled cell identified above, we continue to identify its neighboring cells. For example, we can define I_{i+1} as troubled if $|s_{i+1}| \geq |s_{i-1}|$ and $|s_{i+1}| \geq |s_{i+2}|$ and similarly define I_{i-1} as troubled if $|s_{i-1}| \geq |s_{i-2}|$ and $|s_{i-1}| \geq |s_{i+1}|$. If the cell I_{i-s} and the cell I_{i+r} $(s, r > 0)$ are the first good cells from the left and the right (i.e., I_{i-s+1} and I_{i+r-1} are still troubled cells), we compute the fifth order ENO interpolation polynomial $p_{i-s}(x)$ and $p_{i+r}(x)$ for the cells I_{i-s} and I_{i+r}, respectively. Because of the high order, high resolution WENO scheme (sometimes with anti-diffusive corrector) used in the convection step, r and s will not be larger than 2 in general. The modified cell point value u_i is computed by

$$\tilde{u}_i = \begin{cases} p_{i-s}(x_i), & \theta \geq x_i \\ p_{i+r}(x_i), & \theta < x_i \end{cases}, \tag{10}$$

where the location θ is determined by conservation

$$\int_{x_{i-1/2}}^{\theta} p_{i-s}(x)dx + \int_{\theta}^{x_{i+1/2}} p_{i+r}(x)dx = u_i \, \Delta x. \tag{11}$$

When Δx is sufficiently small, it can be shown that there is a unique θ satisfying Eq. (11) (see [15]). Numerically the unique θ exists in all of our numerical tests. In practice, knowing whether θ is in $[x_{i-1/2}, x_i)$ or $[x_i, x_{i+1/2}]$ is sufficient for obtaining $\tilde{u}_i$. To avoid actually solving θ, we can perform the following simple check: If $F(x_{i-1/2})F(\theta) < 0$, then $\theta < x_i$, where $F(x) = \int_{x_{i-1/2}}^{\theta} p_{i-s}(x)dx + \int_{\theta}^{x_{i+1/2}} p_{i+r}(x)dx - u_i \, \Delta x$.

If there is no solution for θ or there are more than one solution, we choose $\tilde{u}_i = u_{i+r}$. Actually there is no difference to take $\tilde{u}_i$ from left or right for the scalar case because the source term will be zero when $u_i = 0$ or 1. However, in the system case we would like to have the shock travel ahead of the reaction zone, so we take the value of u ahead of the shock.

(3) Use $\tilde{u}_i$ instead of u_i in the ODE solver if the cell I_i is a troubled cell.

For simplicity, consider the Euler forward method

$$u_i^{n+1} = u_i^n + \Delta t S(u_i^n), \tag{12}$$

Eq. (12) is modified to

$$u_i^{n+1} = u_i^n + \Delta t S(\tilde{u}_i), \tag{13}$$

if the cell I_i is a troubled cell.

When extending to a multi-stage Runge-Kutta method, SR is applied for each stage. For example, for second-order Runge-Kutta, at the trouble cell I_i, u_i and $u_i^{(1)}$ are modified to $\tilde{u}_i$ and $\tilde{u}_i^{(1)}$ by SR in the source term:

$$u_i^{(1)} = u_i^n + \Delta t S(\tilde{u}_i), \tag{14}$$

$$u_i^{n+1} = \frac{1}{2}u_i^n + \frac{1}{2}u_i^{(1)} + \frac{1}{2}\Delta t S(\tilde{u}_i^{(1)}). \tag{15}$$

Here we would like to give a remark. Explicit time-stepping methods are used in this paper, because the troubled values u_i^n need to be modified explicitly. Implicit methods, which can hopefully enlarge the time step and improve efficiency, constitute undergoing work. The subcell resolution technique developed in [33] is only designed for the spatial discretization and is frozen during the time step evolution. As the stiffness increases, the CFL number in the reaction step solving the ODE needs to decease in order to obtain a stable solution. See Yee et al. [34] for some studies. In our numerical examples, N_r sub-steps are used in one reaction step, i.e. Eq (8) is modified by

$$U^{n+1} = A\left(\frac{\Delta t}{2}\right) \underbrace{R\left(\frac{\Delta t}{N_r}\right) \cdots R\left(\frac{\Delta t}{N_r}\right)}_{N_r} A\left(\frac{\Delta t}{2}\right) U^n. \tag{16}$$

3 The method for 1D reactive Euler equations with multispecies

In this section, we extend our approach to the 1D reactive Euler equations with multispecies and multireactions.

Consider the reactive Euler equations that model the time-dependent flow of inviscid,

compressible, multispecies reacting flows with n_s species

$$\begin{aligned}
\rho_t + (\rho u)_x &= 0, && (17)\\
(\rho u)_t + (\rho u^2 + p)_x &= 0, && (18)\\
e_t + (u(e+p))_x &= 0, && (19)\\
(\rho z_1)_t + (\rho u z_1)_x &= w_1, && (20)\\
&\dots && (21)\\
(\rho z_{n_s-1})_t + (\rho u z_{n_s-1})_x &= w_{n_s-1}, && (22)
\end{aligned}$$

where ρ is the total density, u is the velocity and e is the total energy. z_m is the mass fraction for the mth species and $\sum_{m=1}^{n_s} z_m = 1$. The pressure p is given by

$$p = (\gamma - 1)\left(e - \frac{1}{2}\rho u^2 - \rho z_1 q_1 - \rho z_2 q_2 - \cdots - \rho z_{n_s} q_{n_s}\right), \quad (23)$$

and the temperature is defined as $T = p/\rho$.

The source term $S(U)$, appearing as w_m in the last equations involving ρz_m, describes the chemical reactions occurring in the gas flows which result in changes in the amount of mass of each chemical species. We assume there are R reactions of the form

$$\nu'_{1,r}X_1 + \nu'_{2,r}X_2 + \cdots + \nu'_{n_s,r}X_{n_s} \to \nu''_{1,r}X_1 + \nu''_{2,r}X_2 + \cdots + \nu_{n_s,r}X_{n_s}, \quad r = 1, \dots, R, \quad (24)$$

where $\nu'_{1,r}$ and $\nu''_{1,r}$ are respectively the stoichiometric coefficients of the reactants and products of species i in the rth reaction. For non-equilibrium chemistry, the rate of production of species i due to chemical reaction may be written as

$$w_i = M_i \sum_{r=1}^{R} (\nu''_{i,r} - \nu'_{i,r}) \left[k_r(T) \prod_{s=1}^{n_s} \left(\frac{\rho_s}{M_s}\right)^{\nu'_{s,r}} \right], \quad i = 1, \dots, n_s. \quad (25)$$

For each reaction r, the reaction rate $k_r(T)$ is assumed to be a known function of the temperature. We consider the Heaviside kinetics form

$$k_r(T) = B_r T^{\alpha_r} H(T - T_r), \quad (26)$$

where $H(x) = 1$ for $x > 0$ and $H(x) = 0$ for $x \le 0$. T_r is the ignition temperature for the rth reaction.

3.1 Convection operator

In the system case, we use the fifth-order WENO with local Lax-Friedrichs flux splitting (WENO-LLF) and the local characteristic decomposition with RK3 for time discretization as the convection operator in the reactive Euler problems. We refer to [20] for more details of this algorithm.

3.2 Reaction operator

The reaction step for the system case is slightly different from the scalar case because there are more component variables involved in the source term. The key point here is to identify transition points correctly and to extrapolate the temperature T and the mass fraction product $\prod_{s=1}^{n_s} {z_s}^{\nu'_{s,r}}$ $(r = 1, \ldots, R)$ in the source term.

(1) We use one mass fraction z to identify transition cells. We take the one with zero value on the left-hand side state. If there is more than one or none, we choose the one with the biggest jump.

We identify the cell I_i as troubled if $|s_i| \geq |s_{i-1}|$ and $|s_i| \geq |s_{i+1}|$ (with at least one strict inequality) where

$$s_i = \text{minmod}\{(z_s)_{i+1} - (z_s)_i, (z_s)_i - (z_s)_{i-1}\}, \tag{27}$$

for a prechosen z_s. Then we continue to identify whether its neighboring cells I_{i-1} and I_{i+1} are troubled cells. For simplicity, in Steps (2) and (3) below, we assume the neighboring cells I_{i-1} and I_{i+1} are not troubled.

(2) After a troubled cell I_i is identified, first find the shock location θ by solving the conservation Eq. (11) with the variable u taken as the total energy E

$$\int_{x_{i-1/2}}^{\theta} p_{i-1}(x; E)dx + \int_{\theta}^{x_{i+1/2}} p_{i+1}(x; E)dx = E_i \, \Delta x, \tag{28}$$

where the ENO interpolation polynomials $p_i(x; E)$ are computed based on values of E. The energy E is chosen because it is a conserved variable. We assume the shock locations are the same for all variables.

Then we extrapolate the temperature T and the mass fraction product in the reaction $\Pi_r = \prod_{s=1}^{n_s} {z_s}^{\nu'_{s,r}}$ $(r = 1, \ldots, R)$ separately. The new mass fraction product $\tilde{\Pi}_r$ $(r = 1, \ldots, R)$ and temperature $\tilde{T}$ are obtained from the ENO interpolation polynomials.

$$\begin{cases} (\tilde{\Pi}_r)_i = p_{i-1}(x_i; \Pi_r), r = 1, \ldots, R, \quad \tilde{T}_i = p_{i-1}(x_i; T), \quad \text{if } \theta \geq x_i \\ (\tilde{\Pi}_r)_i = p_{i+1}(x_i; \Pi_r), r = 1, \ldots, R, \quad \tilde{T}_i = p_{i+1}(x_i; T), \quad \text{if } \theta < x_i \end{cases}. \tag{29}$$

(3) For simplicity, we use the explicit Euler method as the ODE solver in the reaction step

$$(\rho z_s)_i^{n+1} = (\rho z_s)_i^n + \Delta t w_s(\tilde{T}_i, \tilde{\rho}_i, (\tilde{z_1})_i, \ldots, (\tilde{z_{n_s}})_i), \quad s = 1, \ldots, n_s - 1. \tag{30}$$

4 Extension to 2D reactive Euler equations with multispecies

Next, we extend the proposed method to the two-dimensional reactive Euler equations. The considered two-dimensional problem is the extension of the one-dimensional prob-

lem. Consider the reactive Euler equations that model the time-dependent flow of inviscid, compressible, multispecies reacting flows with n_s species

$$U_t + F(U)_x + G(U)_y = S(U). \tag{31}$$

Here U, $F(U)$ and $S(U)$ are column vectors with $m = n_s + 3$ components

$$U = (\rho, \rho u, \rho v, e, \rho z_1, \ldots, \rho z_{n_s-1})^T, \tag{32}$$

$$F(U) = (\rho u, \rho u^2 + p, \rho uv, (e+p)u, \rho z_1 u, \ldots, \rho z_{n_s-1} u)^T, \tag{33}$$

$$G(U) = (\rho v, \rho uv, \rho v^2 + p, (e+p)v, \rho z_1 v, \ldots, \rho z_{n_s-1} v)^T, \tag{34}$$

$$S(U) = (0, 0, 0, 0, w_1, \ldots, w_{n_s-1})^T, \tag{35}$$

where ρ is the total density, u is the x-component velocity, v is the y-component velocity and e is the total energy. The pressure p is

$$p = (\gamma - 1)\left(e - \frac{1}{2}\rho(u^2 + v^2) - \rho z_1 q_1 - \rho z_2 q_2 - \cdots - \rho z_{n_s} q_{n_s}\right)$$

and the temperature is $T = p/\rho$. The source term is the same as that for the 1D reactive Euler system (24) and (25).

In the convection step, we use fifth-order WENO-LLF with RK3 time discretization.

In the reaction step, we apply the subcell resolution procedure dimension by dimension.

(1) Identify the transition points by the shock indicator in both x- and y-directions.

Define the cell I_{ij} as troubled in the x-direction if $|s^x_{ij}| \geq |s^x_{i-1,j}|$ and $|s^x_{ij}| \geq |s^x_{i+1,j}|$ with at least one strict inequality where

$$s^x_{ij} = \text{minmod}\{u_{i+1,j} - u_{ij}, u_{ij} - u_{i-1,j}\}. \tag{36}$$

Similarly we can define the cell I_{ij} as troubled in the y-direction if $|s^y_{ij}| \geq |s^y_{i,j-1}|$ and $|s^y_{ij}| \geq |s^y_{i,j+1}|$ with at least one strict inequality where

$$s^y_{ij} = \text{minmod}\{u_{i,j+1} - u_{ij}, u_{ij} - u_{i,j-1}\}. \tag{37}$$

If I_{ij} is only troubled in one direction, we apply the subcell resolution along this direction. If I_{ij} is troubled in both directions, we choose the direction which has a larger jump. Namely, if $|s^x_{ij}| \geq |s^y_{ij}|$, subcell resolution is applied along the x-direction, otherwise it is done along the y-direction.

In the following steps (2)-(3), without loss of generality, we assume the subcell resolution is applied in the x-direction.

(2) Modify the mass fraction product in the reaction $\prod_{s=1}^{n_s} {z_s}^{\nu'_{s,j}}$ $(r = 1, \ldots, R)$, T_{ij} and ρ_{ij} in the troubled cell I_{ij} by the ENO interpolation polynomials according to the location θ. The location θ is determined by the conservation of energy E

$$\int_{x_{i-1/2}}^{\theta} p_{i-1,j}(x; E)dx + \int_{\theta}^{x_{i+1/2}} p_{i+1,j}(x; E)dx = E_{ij}\Delta x. \tag{38}$$

The treatment of the situation where θ satisfying (38) does not exist is the same as in the 1D case.

(3) For simplicity, explicit Euler is used as the ODE solver in the numerical tests.

$$(\rho z_s)_{ij}^{n+1} = (\rho z_s)_{ij}^{n} + \Delta t w_s(\tilde{T}_{ij}, \tilde{\rho}_{ij}, (\tilde{z_1})_{ij}, \ldots, (\tilde{z_{n_s}})_{ij}), \quad s = 1, \ldots, n_s - 1. \tag{39}$$

5 Numerical examples

In this section, we test the proposed method on both one-dimensional and two-dimensional detonation waves. The proposed method uses a fifth-order WENO-LLF with RK3 as the convection operator, and an explicit Euler based on the subcell resolution as the reaction operator, denoted by WENO5/SR. For most of the examples, we compare the numerical results with the splitting WENO method. The splitting WENO5 denotes the Strang splitting fifth-order WENO method using the local Lax-Friedrichs Flux with RK3 as the convection operator, and an explicit Euler as the reaction operator. For all the one-dimensional examples, the reference solutions are computed by regular fifth-order WENO-LLF (without Strang splitting) with RK3 with $10,000$ grids and CFL=0.5. In all the one-dimensional examples, we have used the positivity-preserving limiter [18] to enhance numerical stability. Notice that this limiter does not affect the high order accuracy of the scheme away from vacuum, as shown in [18]. No cut off safeguard (e.g. cut off the densities which are outside the permissible range) is used in any example.

Example 5.1. A 1D detonation wave with 3 species and 1 reaction.

In the first example, we consider a reacting model with three species and one reaction. This example was studied in [3]. Consider the reaction model

$$2H_2 + O_2 \rightarrow 2H_2O.$$

The parameters are $T_1 = 2.0, B_1 = 500, \alpha_1 = 1, q_1 = 1000, q_2 = 0, q3 = 0, M_1 = 2, M_2 = 32, M_3 = 18$. Initially there is mixture of hydrogen and oxygen on the right-hand side. On the left-hand side, the hydrogen and oxygen generate water. The initial data are

$$(\rho, u, p, z_1, z_2, z_3)(x, 0) = \begin{cases} (\rho_l, u_l, p_l, (z_1)_l, (z_2)_l, (z_3)_l) & x \leq 2.5, \\ (\rho_r, u_r, p_r, (z_1)_r, (z_2)_r, (z_3)_r) & x > 2.5, \end{cases} \tag{40}$$

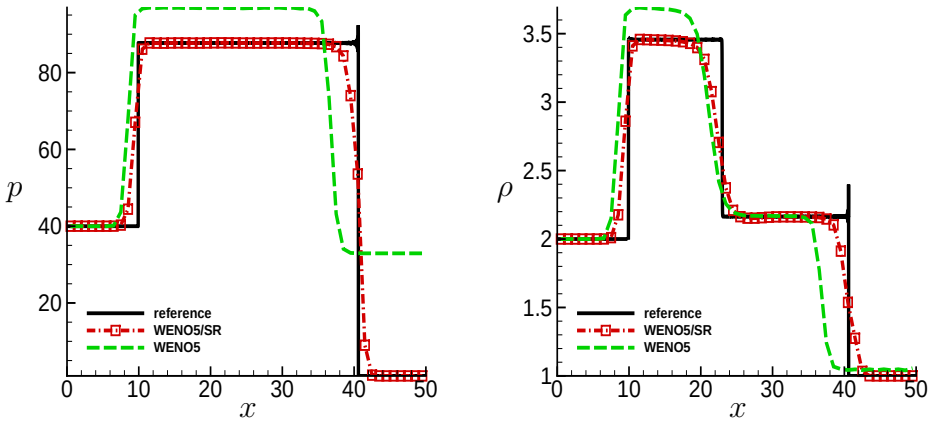

Figure 1: Numerical solutions of Example 5.1 at $t = 3$ with $N = 50$, CFL=0.1, $N_r = 100$. Solid line: reference solution. Red dashed dot line with symbols: WENO5/SR. Green dashed line: splitting WENO5. Left: pressure. Right: density.

where $\rho_l = 2, u_l = 10, p_l = 40, (z_1)_l = 0.325, (z_2)_l = 0, (z_3)_l = 0.625$ and $\rho_r = 1, u_r = 0, p_r = 1, (z_1)_r = 0.4, (z_2)_r = 0.6, (z_3)_r = 0$. The computational domain is $[0, 50]$.

The exact solution consists of a detonation wave, followed by a contact discontinuity and a shock, all moving to the right. We compare the results obtained by the proposed WENO5/SR method and the splitting WENO5 using the same mesh $N = 50$ ($\Delta x = 1$), CFL=0.1 and $N_r = 100$.

Figures 1-3 show the pressure, density, temperature and mass fractions comparison results between the proposed WENO5/SR (red dashed dot line) and the splitting WENO5 (green dashed line), against the reference "exact" solution. Clearly, the proposed WENO5/SR method is able to capture the correct propagation speed of the detonation wave with this coarse mesh, while the splitting WENO5 produces spurious numerical results.

Example 5.2. A 1D detonation wave with 4 species and 1 reaction.

In this example, we test our method on a reacting model with four species and one reaction. A prototype reaction for this model is

$$CH_4 + 2O_2 \rightarrow CO_2 + 2H_2O.$$

This example was also studied in [3].

The parameters are $T_1 = 2.0, B_1 = 10^6, \alpha_1 = 0, q_1 = 500, q_2 = 0, q3 = 0, q_4 = 0, M_1 = 16, M_2 = 32, M_3 = 44, M_4 = 18$. The initial data are given by

$$(\rho, u, p, z_1, z_2, z_3, z_4)(x, 0) = \begin{cases} (\rho_l, u_l, p_l, (z_1)_l, (z_2)_l, (z_3)_l, (z_4)_l) & x \leq 2.5, \\ (\rho_r, u_r, p_r, (z_1)_r, (z_2)_r, (z_3)_r, (z_4)_r) & x > 2.5, \end{cases} \tag{41}$$

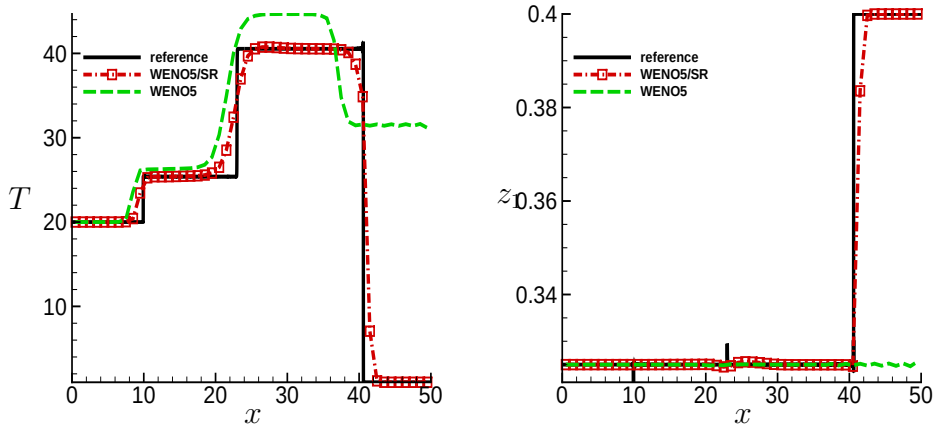

Figure 2: Numerical solutions of Example 5.1 at $t = 3$ with $N = 50$, CFL=0.1, $N_r = 100$. Solid line: reference solution. Red dashed dot line with symbols: WENO5/SR. Green dashed line: splitting WENO5. Left: temperature. Right: mass fraction of z_1.

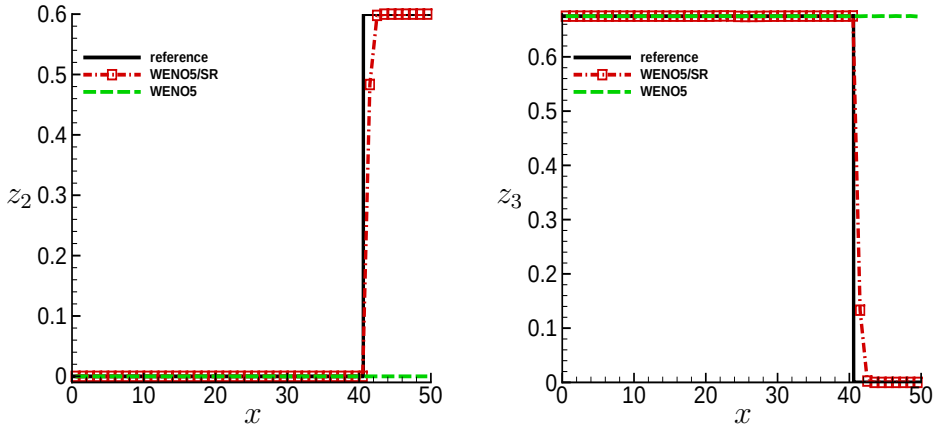

Figure 3: Numerical solutions of Example 5.1 at $t = 3$ with $N = 50$, CFL=0.1, $N_r = 100$. Solid line: reference solution. Red dashed dot line with symbols: WENO5/SR. Green dashed line: splitting WENO5. Left: mass fraction of z_2. Right: mass fraction of z_3.

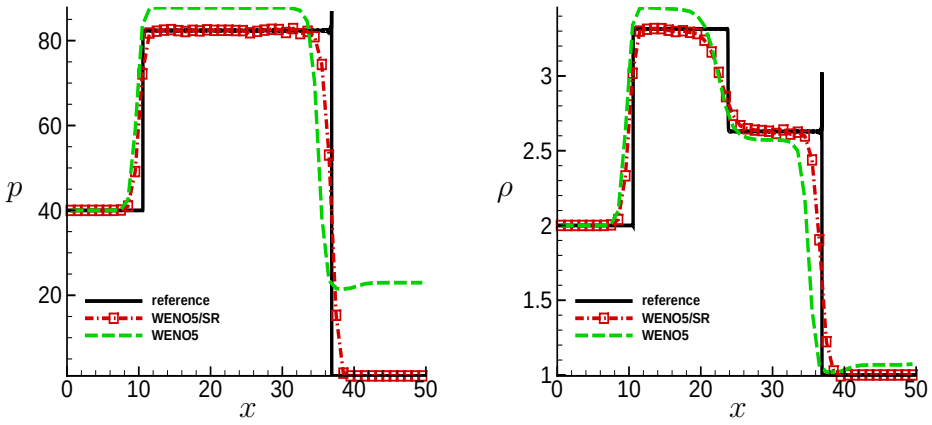

Figure 4: Numerical solutions of Example 5.2 at $t = 3$ with $N = 50$, CFL=0.1, $N_r = 100$. Solid line: reference solution. Red dashed dot line with symbols: WENO5/SR. Green dashed line: splitting WENO5. Left: pressure. Right: density.

where $\rho_l = 2, u_l = 10, p_l = 40, (z_1)_l = 0, (z_2)_l = 0.2, (z_3)_l = 0.475, (z_4)_l = 0.325$ and $\rho_r = 1, u_r = 0, p_r = 1, (z_1)_r = 0.1, (z_2)_r = 0.6, (z_3)_r = 0.2, (z_4)_r = 0.1$. The computational domain is $[0, 50]$. The exact solution consists of a detonation wave, followed by a contact discontinuity and a shock, all moving to the right.

Figures 4-6 show the pressure, density, temperature and mass fractions comparison results between the proposed WENO5/SR method (red dashed dot line) and the splitting WENO5 (green dashed line), against the reference "exact" solution, using the same mesh $N = 50$ ($\Delta x = 1$), CFL=0.1 and $N_r = 100$. Again, the proposed WENO5/SR method is able to capture the correct propagation speed of the detonation wave with this coarse mesh, while the splitting WENO5 produces spurious numerical results.

Example 5.3. A 1D detonation wave with 5 species and 2 reactions.

In the last one-dimensional example, we consider the reactive Euler system with multireactions. Consider

$$H_2 + O_2 \rightarrow 2OH, \quad 2OH + H_2 \rightarrow 2H_2O,$$

with N_2 appearing as a catalyst. In this example, there are five species and two reactions. The parameters are $T_1 = 2.0, T_2 = 10, B_1 = B_2 = 10^6, \alpha_1 = \alpha_2 = 0, q_1 = 0, q_2 = 0, q3 = -20, q_4 = -100, q_5 = 0, M_1 = 2, M_2 = 32, M_3 = 17, M_4 = 18, M_5 = 28$. We use similar parameters as those in [3] except that we increase the reacting rate B_1 and B_2 ten times larger for more stiffness.

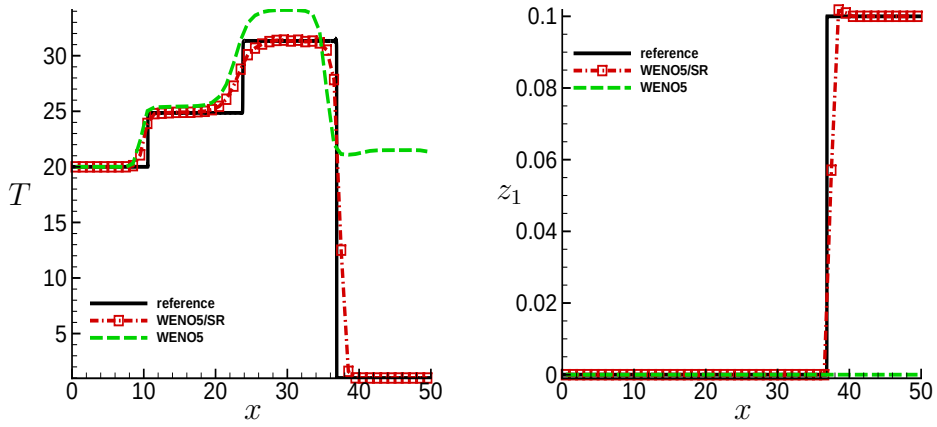

Figure 5: Numerical solutions of Example 5.2 at $t = 3$ with $N = 50$, CFL=0.1, $N_r = 100$. Solid line: reference solution. Red dashed dot line with symbols: WENO5/SR. Green dashed line: splitting WENO5. Left: temperature. Right: mass fraction of z_1.

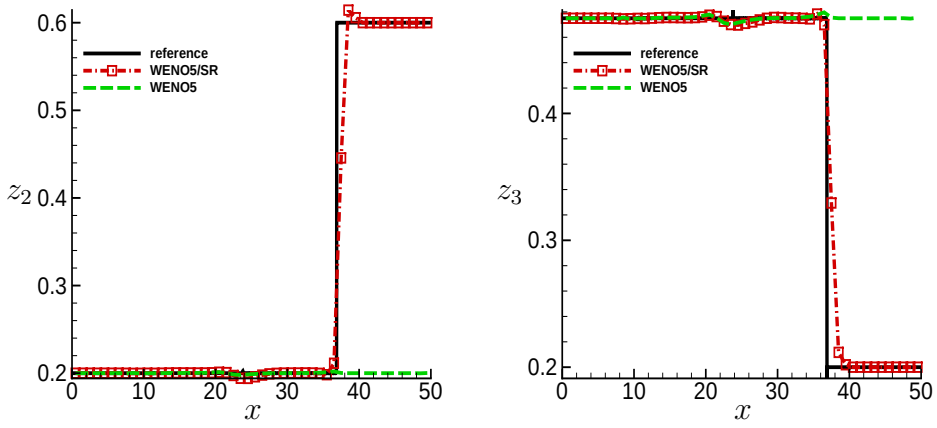

Figure 6: Numerical solutions of Example 5.2 at $t = 3$ with $N = 50$, CFL=0.1, $N_r = 100$. Solid line: reference solution. Red dashed dot line with symbols: WENO5/SR. Green dashed line: splitting WENO5. Left: mass fraction of z_2. Right: mass fraction of z_3.

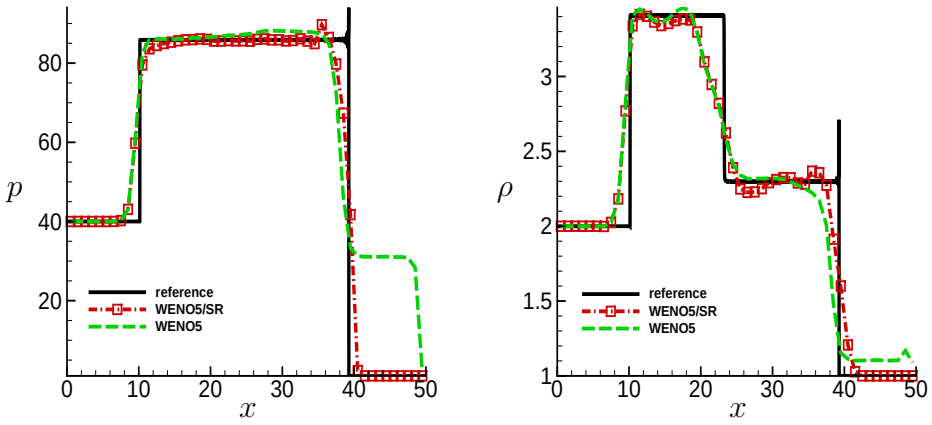

Figure 7: Numerical solutions of Example 5.3 at $t = 3$ with $N = 50$, CFL=0.05, $N_r = 400$. Solid line: reference solution. Red dashed dot line with symbols: WENO5/SR. Green dashed line: splitting WENO5. Left: pressure. Right: density.

The initial data are

$$(\rho, u, p, z_1, z_2, z_3, z_4, z_5)(x, 0) = \begin{cases} (\rho_l, u_l, p_l, (z_1)_l, (z_2)_l, (z_3)_l, (z_4)_l, (z_5)_l) & x \le 2.5, \\ (\rho_r, u_r, p_r, (z_1)_r, (z_2)_r, (z_3)_r, (z_4)_r, (z_5)_r) & x > 2.5, \end{cases} \tag{42}$$

where $\rho_l = 2, u_l = 10, p_l = 40, (z_1)_l = 0, (z_2)_l = 0, (z_3)_l = 0.17, (z_4)_l = 0.63, (z_5)_l = 0.2$, and $\rho_r = 1, u_r = 0, p_r = 1, (z_1)_r = 0.08, (z_2)_r = 0.72, (z_3)_r = 0, (z_4)_r = 0, (z_5)_r = 0.2$. The computational domain is $[0, 50]$. The exact solution consists of a detonation wave, followed by a rarefaction wave and a shock, all moving to the right. We compare the results obtained by the proposed WENO5/SR method and the splitting WENO5, against the reference "exact" solution, using the same mesh $N = 50$ ($\Delta x = 1$), CFL=0.05 and $N_r = 400$. Figures 7-9 show the pressure, density, temperature and mass fractions comparison results between the proposed WENO5/SR method (red dashed dot line) and the splitting WENO5 (green dashed line). From all the results, the proposed WENO5/SR method is able to capture the correct shock location in coarse mesh, but the regular WENO method produces spurious wave from the location $x = 40$. We remark that unlike the one reaction examples, the proposed WENO5/SR scheme needs a smaller CFL number (about one half for the present example) for stability compared to the splitting WENO5 in this multireaction example.

Example 5.4. A 2D detonation wave with 4 species and 1 reaction.

Now we test our method on two-dimensional problems. The first two-dimensional example is one with radial symmetry analogous to Example 5.2. The same example was

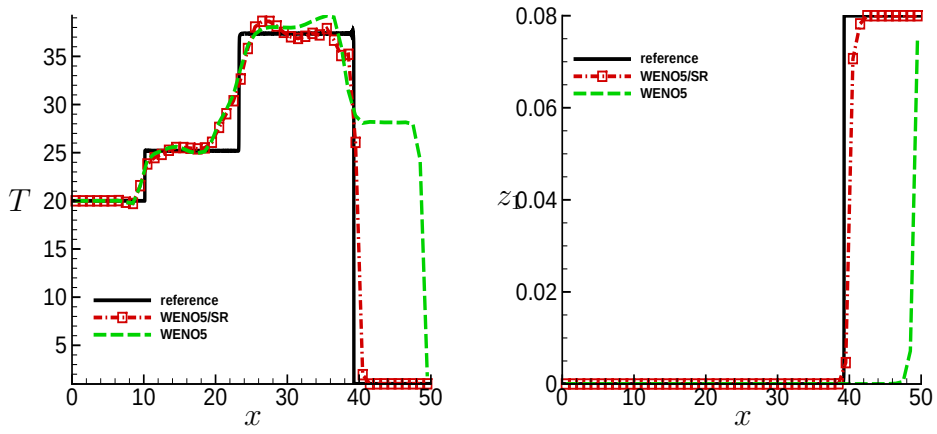

Figure 8: Numerical solutions of Example 5.3 at $t = 3$ with $N = 50$, CFL=0.05, $N_r = 400$. Solid line: reference solution. Red dashed dot line with symbols: WENO5/SR. Green dashed line: splitting WENO5. Left: temperature. Right: mass fraction of z_1.

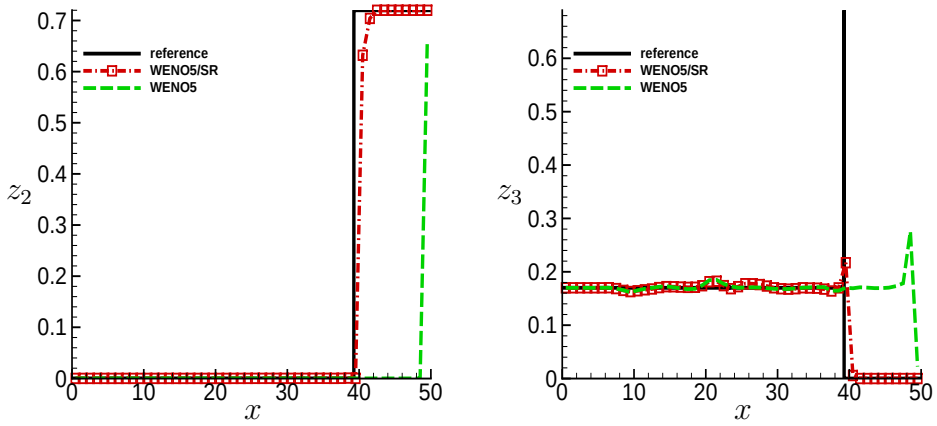

Figure 9: Numerical solutions of Example 5.3 at $t = 3$ with $N = 50$, CFL=0.05, $N_r = 400$. Solid line: reference solution. Red dashed dot line with symbols: WENO5/SR. Green dashed line: splitting WENO5. Left: mass fraction of z_2. Right: mass fraction of z_3.

studied in [3] and a similar one with two species was studied in [16]. The parameters $T_1, B_1, \alpha_1, q_1, q_2, q_3, q_4$ are the same as those in Example 5.2 except $q_1 = 200$. The initial values consist of totally burnt gas inside of a circle with radius 10 and totally unburnt gas everywhere outside this circle. The set up is as follows

$$(\rho, u, v, p, z_1, z_2, z_3, z_4)(x, y, 0) = \begin{cases} (\rho_l, u_l, v_l, p_l, (z_1)_l, (z_2)_l, (z_3)_l, (z_4)_l) & r \le 10, \\ (\rho_r, u_r, v_r, p_r, (z_1)_r, (z_2)_r, (z_3)_r, (z_4)_r) & r > 10, \end{cases} \tag{43}$$

where $r = \sqrt{x^2 + y^2}, \rho_l = 2, u_l = 10x/r, v_l = 10y/r, p_l = 40, (z_1)_l = 0, (z_2)_l = 0.2, (z_3)_l = 0.475, (z_4)_l = 0.325$ and $\rho_r = 1, u_r = 0, v_r = 0, p_r = 1, (z_1)_r = 0.1, (z_2)_r = 0.6, (z_3)_r = 0.2, (z_4)_r = 0.1$. The computational domain is $[0, 50] \times [0, 50]$.

This is a radially symmetric problem and the detonation front is circular. The boundary conditions are solid-wall boundary conditions on the left and lower boundaries and outflow boundary conditions on the right and upper boundaries. Figures 10-11 show the pressure, density and mass fractions z_1 and z_2 at $t = 2$. We compare the results between the proposed WENO5/SR method and the splitting WENO5 using the same mesh size $N_x \times N_y = 25 \times 25$ ($\Delta x = \Delta y = 2$), CFL=0.1 and $N_r = 100$. The reference solution is computed by standard WENO5 scheme with a mesh of 1000×1000 grid points. The proposed scheme clearly has captured the detonations well in the coarse mesh, however the regular WENO scheme produces spurious waves in all figures. Figures 12 and 13 show the velocity contour by the proposed WENO5/SR scheme at four different times $t = 1, 2, 4$ and 6. We can see the circular detonation front moving nicely. There is no spurious nonphysical wave generated.

Example 5.5. A 2D detonation wave with 5 species and 2 reactions.

The second 2D example is the 2D case analogous to Example 5.3 with 5 species and 2 reactions. The parameters $T_1, T_2, B_1, B_2, \alpha_1, \alpha_2, q_1, q_2, q_3, q_4, q_5$ are the same as those in Example 5.3. The initial condition is given by

$$(\rho, u, v, p, z_1, z_2, z_3, z_4, z_5)(x, y, 0) = \begin{cases} (\rho_l, u_l, v_l, p_l, (z_1)_l, (z_2)_l, (z_3)_l, (z_4)_l, (z_5)_l) & x \le \xi(y), \\ (\rho_r, u_r, v_r, p_r, (z_1)_r, (z_2)_r, (z_3)_r, (z_4)_r, (z_5)_r) & x > \xi(y), \end{cases} \tag{44}$$

where

$$\xi(y) = \begin{cases} 12.5 - |y - 12.5|, & |y - 12.5| \le 7.5, \\ 5, & |y - 12.5| > 7.5, \end{cases} \tag{45}$$

and $\rho_l = 2, u_l = 10, v_l = 0, p_l = 40, (z_1)_l = 0, (z_2)_l = 0, (z_3)_l = 0.17, (z_4)_l = 0.63, (z_5)_l = 0.2$ and $\rho_r = 1, u_r = 0, v_r = 0, p_r = 1, (z_1)_r = 0.08, (z_2)_r = 0.72, (z_3)_r = 0, (z_4)_r = 0, (z_5)_r = 0.2$. The computational domain is $[0, 150] \times [0, 25]$. The inflow boundary conditions are used on the left boundary and the outflow boundary conditions are used on the right boundary. The top and bottom boundaries are solid walls. The same example was studied in [3]. A similar problem with 2-species was computed in our

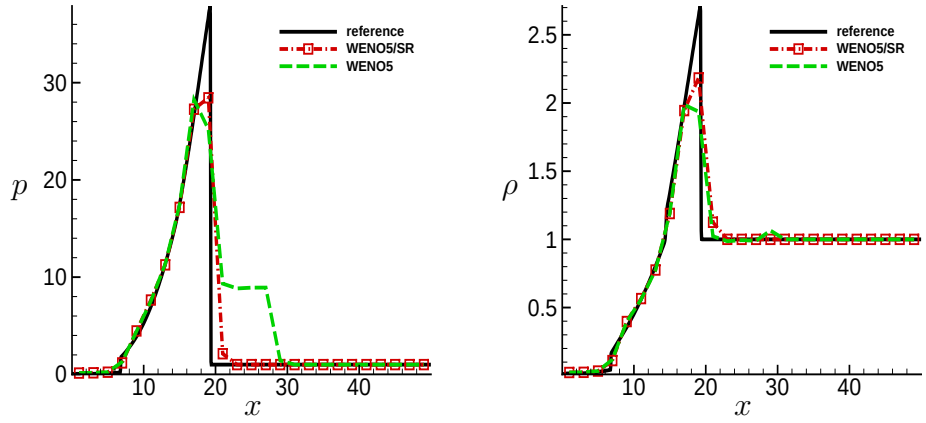

Figure 10: Numerical solutions of Example 5.4 at $t = 2$ with $N_x \times N_y = 25 \times 25$, CFL=0.1, $N_r = 100$. Solid line: reference solution. Red dashed dot line with symbols: WENO5/SR. Green dashed line: splitting WENO5. Left: pressure. Right: density.

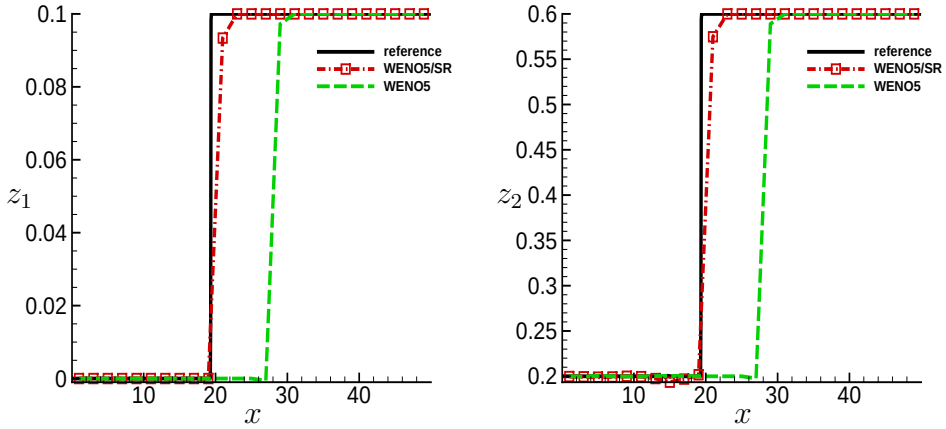

Figure 11: Numerical solutions of Example 5.4 at $t = 2$ with $N_x \times N_y = 25 \times 25$, CFL=0.1, $N_r = 100$. Solid line: reference solution. Red dashed dot line with symbols: WENO5/SR. Green dashed line: splitting WENO5. Left: mass fraction of z_1. Right: mass fraction of z_2.

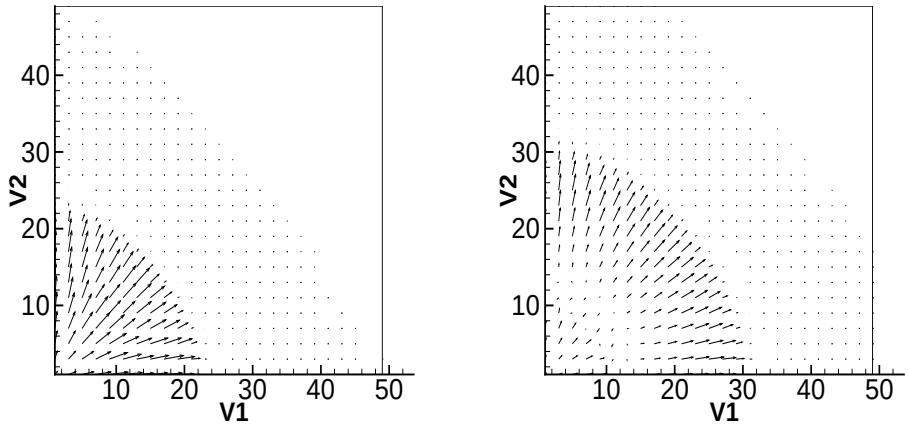

Figure 12: Numerical solutions of Example 5.4 by WENO5/SR with $N_x \times N_y = 25 \times 25$, CFL=0.1, $N_r = 100$. Velocity fields. Left: at $t = 1$. Right: at $t = 2$.

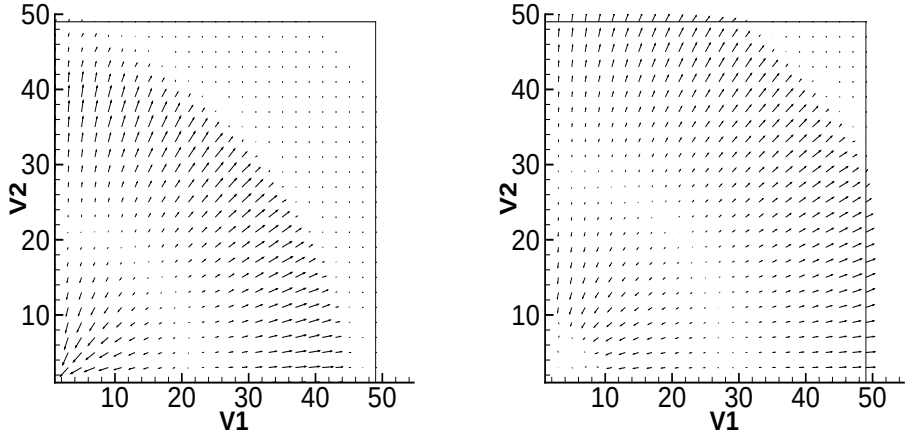

Figure 13: Numerical solutions of Example 5.4 by WENO5/SR with $N_x \times N_y = 25 \times 25$, CFL=0.1, $N_r = 100$. Velocity fields. Left: at $t = 4$. Right: at $t = 6$.

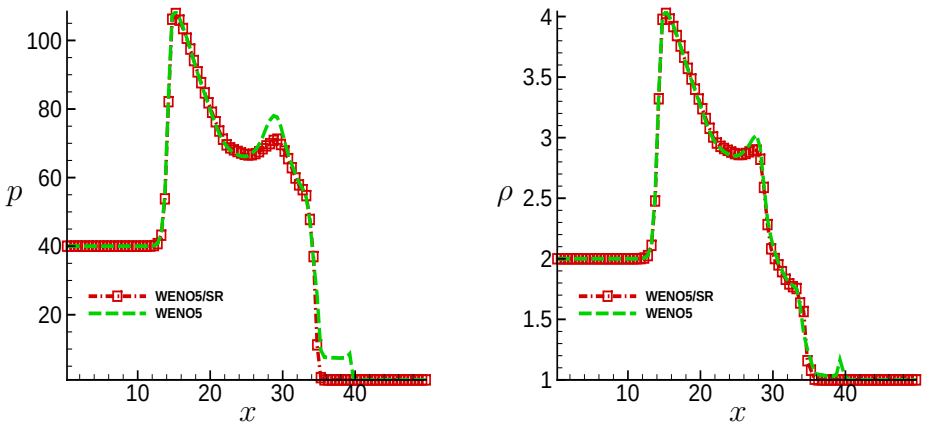

Figure 14: Numerical solutions by WENO5/SR of Example 5.5 at $t = 2$ with 100×51 on domain $[0, 50] \times [0, 25]$, CFL=0.1, $N_r = 100$. Solid line: reference solution. Red dashed dot line with symbols: WENO5/SR. Green dashed line: splitting WENO5. Left: pressure. Right: density.

previous work [33]. One important feature of this solution is the appearance of triple points, which travel along the detonation front in the transverse direction and reflect from the upper and lower walls, forming a cellular pattern. Behind the detonation front, there is a strong shock.

We first show the comparison of WENO5/SR and splitting WENO5 with the same mesh size $\Delta x = \Delta y = 0.5$, CFL=0.1 and $N_r = 100$ at the 1D cross section $y = 12.5$ at $t = 2$ in Figures 14 and 15. Since at $t = 2$ the flow has not touched $x = 50$, the results are computed on the cutoff computational domain $[0, 50] \times [0, 25]$ with $N_x \times N_y = 100 \times 51$. It is easy to see from the pressure, temperature and mass fraction results that the regular WENO scheme already produces spurious waves (around $x = 35$ to $x = 40$) at $t = 2$.

Next, the density contours are computed by WENO5/SR with the mesh $N_x \times N_y = 300 \times 51$ (same mesh size $\Delta x = \Delta y = 0.5$) on the whole domain $[0, 150] \times [0, 25]$. Figure 16 show the results at nine evolutionary times from $t = 0$ to $t = 8$. It is clear that there are no spurious waves in the wave front by our proposed scheme.

6 Concluding remarks

In this paper, we extend our previous work [33] of SR from two species single-reaction to multi-species multi-reaction, which is significantly more difficult because of the multiple scales generated by different reactions. The proposed scheme is a fractional scheme

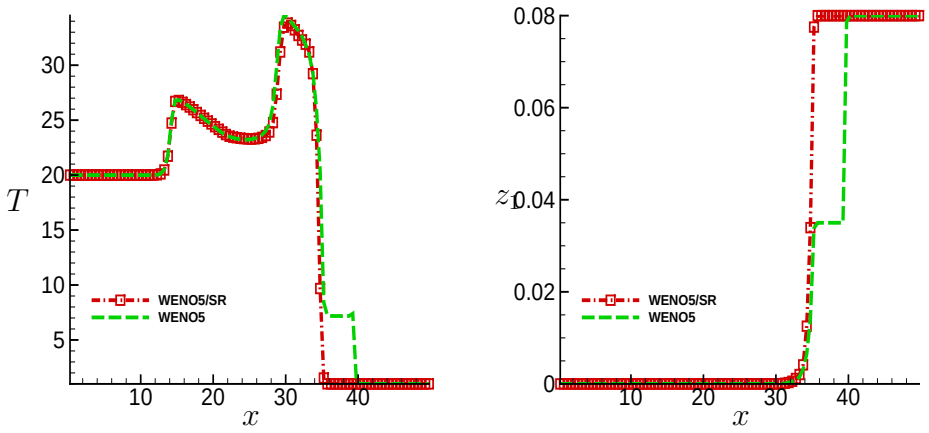

Figure 15: Numerical solutions by WENO5/SR of Example 5.5 at $t = 2$ with 100×51 on domain $[0, 50] \times [0, 25]$, CFL=0.1, $N_r = 100$. Solid line: reference solution. Red dashed dot line with symbols: WENO5/SR. Green dashed line: splitting WENO5. Left: temperature. Right: mass fraction of z_1.

with the flexibility of choosing any spatial high-order shock-capturing scheme in the convection step. In the reaction step, any explicit ODE solver can be used with the transition points reconstructed by Harten's ENO subcell resolution idea. The method has high order accuracy in space for smooth flows. It is able to capture the correct location of discontinuity in very coarse mesh. We remark that our method can use fewer points than the previous methods in [3] to obtain similar results for the similar examples. The reason may be due to the high order accuracy of the spatial scheme in the convection step.

Although the underresolved temporal mesh problem is not solved, as the stiffness increases, small time step is only needed for the reaction step with more sub-steps. Ongoing work is to investigate implicit time discretization in the ODE step to address this small time step issue.

For more complex fully coupled multi-species and multi-reaction flows, further investigations are needed. For example, in a 13-species and multi-reaction hypersonic simulation on a hypersonic spacecraft earth-entry-like condition simulation, the relative distance between the shear/contact and shock is different from one grid spacing to another as well as their discontinuity locations for each numerical method indicated in Kotov et al. [21]. This spurious behavior of shock-capturing methods has not appeared in the literature.

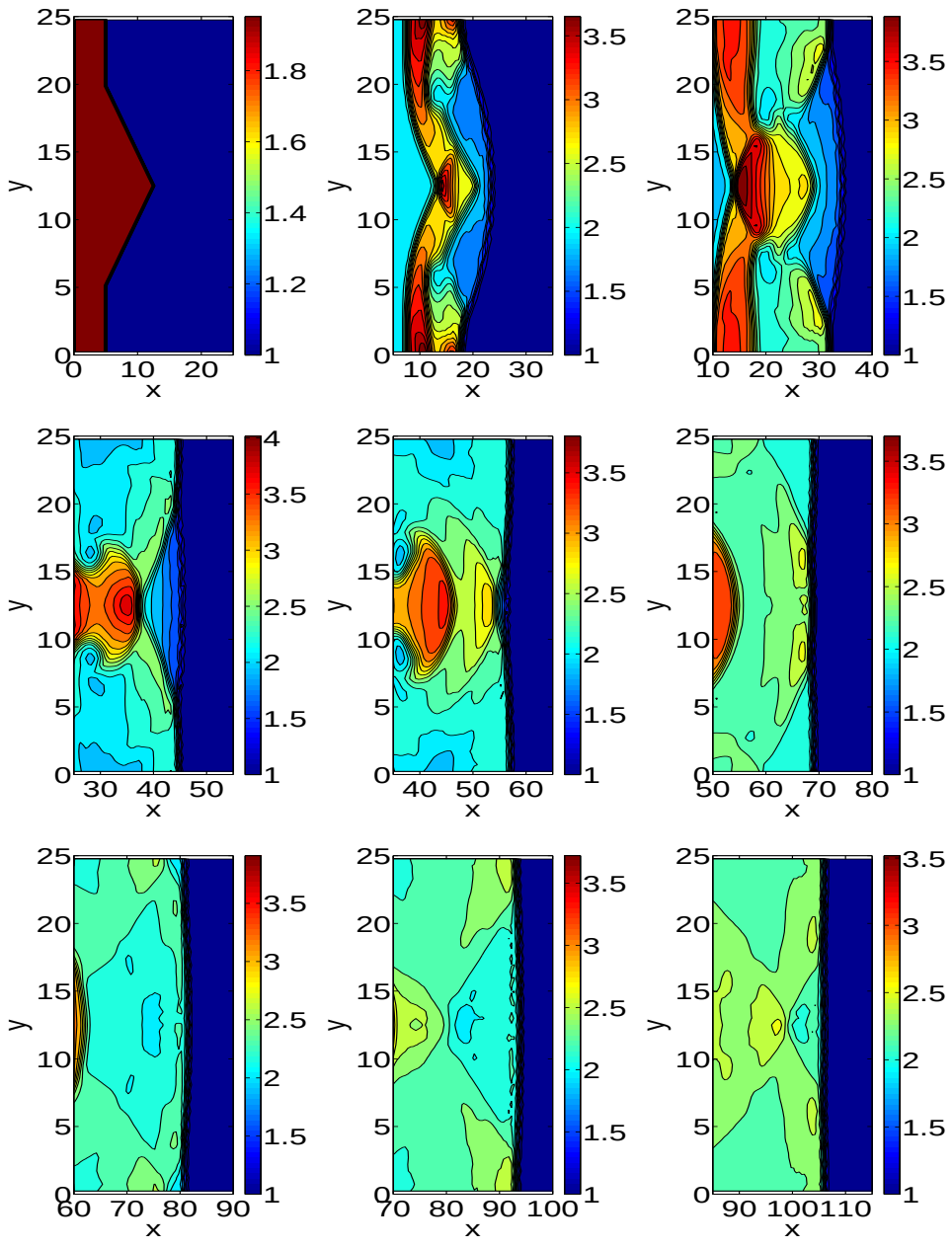

Figure 16: Computed density for Example 5.5: WENO5/SR with 300×51 on domain $[0, 150] \times [0, 25]$, CFL=0.05 and $N_r = 100$ at nine different evolutionary times from $t = 0$ to $t = 8$.

References

[1] W. Bao and S. Jin. The random projection method for hyperbolic conservation laws with stiff reaction terms. *J. Comput. Phys.*, 163:216–248, 2000.

[2] W. Bao and S. Jin. The random projection method for stiff detonation capturing. *SIAM J. Sci. Comput.*, 23:1000–1025, 2001.

[3] W. Bao and S. Jin. The random projection method for stiff multispecies detonation capturing. *J. Comput. Phys.*, 178:37–57, 2002.

[4] M. Ben-Artzi. The generalized Riemann problem for reactive flows. *J. Comput. Phys.*, 81:70–101, 1989.

[5] A. Berkenbosch, E. Kaasschieter and R. Klein. Detonation capturing for stiff combustion chemistry. *Combust. Theory Model.*, 2:313–348, 1998.

[6] B. Bihari and D. Schwendeman. Multiresolution schemes for the reactive euler equations. *J. Comput. Phys.*, 154:197–230, 1999.

[7] A. Bourlioux, A. Majda and V. Roytburd. Theoretical and numerical structure for unstable one-dimensional detonations. *SIAM J. Appl. Math.*, 51:303–343, 1991.

[8] S.-H. Chang. On the application of subcell resolution to conservation laws with stiff source terms. *NASA Technical Memorandum 102384, ICOMP Report 89-27*, 1989.

[9] S.-H. Chang. On the application of subcell resolution to conservation laws with stiff source terms. *NASA Lewis Research Center, Computational Fluid Dynamics Symposium on Aeropropulsion*, 215–225, 1991.

[10] A. Chorin. Random choice solution of hyperbolic systems. *J. Comput. Phys.*, 22:517–533, 1976.

[11] A. Chorin. Random choice methods with applications for reacting gas flows. *J. Comput. Phys.*, 25:253–272, 1977.

[12] P. Colella, A. Majda and V. Roytburd. Theoretical and numerical structure for numerical reacting waves. *SIAM J. Sci. Stat. Comput.*, 7:1059–1080, 1986.

[13] B. Engquist and B. Sjögreen. Robust difference approximations of stiff inviscid detonation waves. *Technical Report CAM 91-03, UCLA.*, 1991.

[14] D. Griffiths, A. Stuart and H. C. Yee. Numerical wave propagation in an advection equation with a nonlinear source term. *SIAM J. Numer. Anal.*, 29:1244–1260, 1992.

[15] A. Harten. ENO schemes with subcell resolution. *J. Comput. Phys.*, 83:148–184, 1989.

[16] C. Helzel, R. LeVeque and G. Warneke. A modified fractional step method for the accurate approximation of detonation waves. *SIAM J. Sci. Stat. Comput.*, 22:1489–1510, 1999.

[17] A. Hidalgo and M. Dumbser. ADER schemes for nonlinear systems of stiff advection-diffusion-reaction equations. *J. Sci. Comput.*, 48:173–189, 2011.

[18] X.Y. Hu, N.A. Adams, and C.-W. Shu. Positivity-preserving flux limiters for high-order conservative schemes solving compressible Euler equations. *J. Comput. Phys.*, 242:169–180, 2013.

[19] R. Jeltsch and P. Klingenstein. Error estimators for the position of discontinuities in hyperbolic conservation laws with source term which are solved using operator splitting. *Comput. Vis. Sci.*, 1:231–249, 1999.

[20] G Jiang and C.-W. Shu. Efficient implementation of weighted ENO schemes. *J. Comput. Phys.*, 126:202–228, 1996.

[21] D. Kotov, H. C. Yee, M. Panesi, A. Wray, D. Prabhu. 1D and 2D Simulation Related to the NASA Electric Arc Shock Tube Experiments, *21st AIAA Computational Fluid Dynamics Conference, contributed paper*, June 24-27, 2013, San Diego, CA.

[22] R. J. LeVeque and H. C. Yee. A study of numerical methods for hyperbolic conservation laws with stiff source terms. *J. Comput. Phys.*, 86:187–210, 1990.

[23] R.J. LeVeque and K.-M. Shyue. One-dimensional front tracking based on high resolution wave propagation methods. *SIAM J. Sci. Comput.*, 16:348–377, 1995.

[24] A. Majda and V. Roytburd. Numerical study of the mechanisms for initiation of reacting shock waves. *SIAM J. Sci. Stat. Comput.*, 11:950–974, 1990.

[25] F. Miniati and P. Colella. A modified higher order Godunov scheme for stiff source conservative hydrodynamics. *J. Comput. Phys.*, 224:519–538, 2007.

[26] D. Nguyen, F. Gibou and R. Fedkiw. A fully conservative ghost fluid method & stiff detonation waves. *Proceedings of the 12th International Detonation Symposium, San Diego, CA*, 2002.

[27] R. Pember. Numerical methods for hyperbolic conservation laws with stiff relaxation, I. spurious solutions. *SIAM J. Appl. Math.*, 53:1293–1330, 1993.

[28] C.-W. Shu and S. Osher. Efficient implementation of essentially non-oscillatory shock capturing schemes, II. *J. Comput. Phys.*, 83:32–78, 1989.

[29] G. Strang. On the construction and comparison of difference schemes. *SIAM J. Numer. Anal.*, 5:506–517, 1968.

[30] Y. Sun and B. Engquist. Heterogeneous multiscale methods for interface tracking of combustion fronts. *Multiscale Model. Simul.*, 5:532–563, 2006.

[31] V. Ton. Improved shock-capturing methods for multicomponent and reacting flows. *J. Comput. Phys.*, 128:237–253, 1996.

[32] L. Tosatto and L. Vigevano. Numerical solution of under-resolved detonations. *J. Comput. Phys.*, 227:2317–2343, 2008.

[33] W. Wang, C.-W. Shu, H.C. Yee and B. Sjögreen. High order finite difference methods with subcell resolution for advection equations with stiff source terms. *J. Comput. Phys.*, 231:190–214, 2012.

[34] H.C. Yee, D.V. Kotov, W. Wang and C.-W. Shu. Spurious behavior of shock-capturing methods: problems containing stiff source terms and discontinuities. *J. Comput. Phys.*, 241:266–291, 2013.